Communications

Urea Lesion Formation in DNA as a Consequence of 7,8-Dihydro-8-oxoguanine Oxidation and Hydrolysis Provides a Potent Source of Point Mutations

Paul T. Henderson,[†,‡,§] William L. Neeley,[†,§] James C. Delaney,[†] Feng Gu,[†] Jacquine C. Niles,[†] Sang Soo Hah,[‡] Steven R. Tannenbaum,[†] and John M. Essigmann*[,†]

Department of Chemistry and Biological Engineering Division, Massachusetts Institute of Technology, 77 Massachusetts Avenue, Cambridge, Massachusetts 02139, and Biology and Biotechnology Research Program, Lawrence Livermore National Laboratory, Livermore, California 94551

Received August 31, 2004

The DNA oxidation product 7,8-dihydro-8-oxoguanine (8-oxoG) forms several mutagenic oxidation products, including a metastable oxaluric acid (Oa) derivative. We report here that a synthetic oligonucleotide containing Oa hydrolyzes under simulated "in vivo" conditions to form a mutagenic urea (Ua) lesion. Using the Oa 2′-deoxyribonucleoside as a model, the hydrolysis rate depended strongly upon the concentrations of bicarbonate and divalent magnesium. In buffered solutions containing physiologically relevant levels of these species, the half-life of Oa nucleoside was approximately 40 h at 37 °C. The mutagenic properties of Ua in DNA were investigated using a M13mp7L2 bacteriophage genome containing Ua at a specific site. Transfection of the lesion-containing genome into wild-type AB1157 *Escherichia coli* allowed determination of the mutation frequency and DNA polymerase bypass efficiency from the resulting progeny phage. Ua was bypassed with an efficiency of 11% as compared to a guanine control and caused a 99% G→T mutation frequency, assuming the lesion originated from G, which is at least an order of magnitude higher than the mutation frequency of 8-oxoG under the same conditions. SOS induction of bypass DNA polymerase(s) in the bacteria prior to transfection caused the mutation frequency and type to shift to 43% G→T, 46% G→C, and 10% G→A mutations. We suggest that Ua is instructional, meaning that the shape of the lesion and its interactions with DNA polymerases influence which nucleotide is inserted opposite the lesion during replication and that the instructional nature of the lesion is modulated by the size of the binding pocket of the DNA polymerase. Replication past Ua, when formed by hydrolysis of the 8-oxoG oxidation product Oa, denotes a pathway that nearly quantitatively generates point mutations in vivo.

Introduction

DNA damage mediated by reactive oxygen and nitrogen species is believed to contribute to the etiology of human cancer, aging, and neurological disorders (*1*−*3*). Examining the mutagenicity and repair of DNA oxidation products and providing a structural basis for these effects are of fundamental importance for understanding their genotoxic properties. The lesion 7,8-dihydro-8-oxoguanine (8-oxoG)[1] is regarded as perhaps the most critical product resulting from oxidative DNA damage due to its high steady state concentration in cells and a capability to mispair with A, which leads to G→T transversion mutations (*4*−*9*). Recent studies in this laboratory and others have shown that 8-oxoG is an unstable species under a variety of oxidative conditions, owing to its low oxidation potential as compared to the parent 2′-deoxyguanosine (*10*). A variety of DNA lesions is formed when 8-oxoG is exposed to oxidative conditions (*11*−*21*). The product distribution depends on the mechanism of action of the oxidant and the reaction conditions. For example, peroxynitrite ($ONOO^-$), a powerful oxidant that is formed in vivo by the combination of nitric oxide with superoxide (*22*−*24*), reacts preferentially with 8-oxoG as compared to the four canonical nucleobases to form several lesions

* To whom correspondence should be addressed. Tel: 617-253-6227. Fax: 617-253-5445. E-mail: jessig@mit.edu.
† Massachusetts Institute of Technology.
‡ Lawrence Livermore National Laboratory.
§ These authors contributed equally to the manuscript.

[1]Abbreviations: AP, apurinic/apyrimidinic; Ca, cyanuric acid; Gh, guanidinohydantoin; Iz, imidazolone; MALDI-TOF, matrix-assisted laser desorption/ionization time-of-flight; MW, molecular weight; Oa, oxaluric acid; $ONOO^-$, peroxynitrite; 8-oxoG, 7,8-dihydro-8-oxo-2′-deoxyguanine; Oz, oxazalone; PAGE, polyacrylamide gel electrophoresis; PNK, polynucleotide kinase; REAP, restriction endonuclease and postlabeling; Sp, spiroiminodihydantoin; ss, single-stranded; THF, tetrahydrofuran; Ua, urea.

10.1021/tx049757k CCC: $30.25
Published on Web 12/13/2004

Table 1. Summary of Bypass Efficiencies and Mutation Frequencies for 8-OxoG Oxidation Products in WT *E. coli*

	8-oxoG oxidation product							
property	Ca[a]	Iz[b]	Oz[a]	Gh[c]	Sp1[c]	Sp2[c]	Oa[d]	Ua[d]
bypass efficiency (%)	65 ± 8	60 ± 5	57 ± 13	75 ± 5	9 ± 3	9 ± 4	51 ± 3	11 ± 5
G→T mutations (%)	97	1	86	1.4	27	41	99	99
G→C mutations (%)	<1	88	<1	98	72	57	<1	<1
G→A mutations (%)	<1	2	<1	<1	<1	<1	<1	<1

[a] Ref *26*. [b] Ref *28*. [c] Ref *27*. [d] This work.

Scheme 1

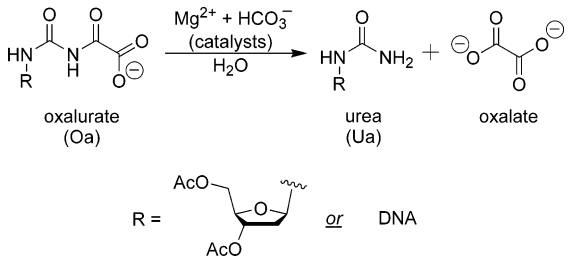

including cyanuric acid (Ca), imidazolone (Iz) and its hydrolysis product oxazalone (Oz), guanidinohydantoin (Gh), spiroiminodihydantoin diastereomers (Sp1 and Sp2), and oxaluric acid (Oa) (*2*). The distribution of the 8-oxoG oxidation products is strongly dependent on the buffer composition and the concentration of $ONOO^-$. For example, Oa, Oz, and Ca are predominantly formed in the presence of a molar excess of $ONOO^-$ and 25 mM sodium bicarbonate in phosphate buffer (pH 7.2) (*20*). In contrast, when $ONOO^-$ is slowly infused over time, the lesions Gh and Sp predominantly form (*25*). We recently reported that these secondary lesions are an order of magnitude more mutagenic than 8-oxoG and that they are well-bypassed by DNA polymerase during replication in *Escherichia coli* (*26*−*28*) (Table 1).

In the course of our studies, we observed that Oa decomposes in aqueous solution to form a urea (Ua) derivative, a DNA base lesion that is usually ascribed to the presence of pyrimidine oxidation. To our knowledge, the formation of Ua during 8-oxoG oxidation has been reported only once (*29*); however, in that study, a 1,3-diamine, such as spermine or 1,3-diaminopropane, was required for the production of Ua. Herein, we describe the hydrolysis of Oa to Ua in 2′-deoxynucleoside and oligonucleotide models at physiologically relevant pH values and salt concentrations (Scheme 1). The effect of normal and SOS-induced cellular conditions on the mutagenic potential of Oa and Ua in DNA was determined in an M13 bacteriophage system using the recently developed restriction endonuclease and postlabeling (REAP) assay (Figure 1) (*30*−*32*). The hydrolysis and mutation results support a novel potential pathway to mutagenesis in vivo from the oxidation of 8-oxoG.

Materials and Methods

Chemicals and Enzymes. Restriction endonucleases, T4 polynucleotide kinase (PNK), and T4 DNA ligase were purchased from New England Biolabs. M13mp7L2 was a gift from C. W. Lawrence (University of Rochester). The *E. coli* cell strain used for transfection was AB1157, and for plating, it was NR9050 from R. M. Schaaper (NIEHS). The *E. coli* strain used for regrowth of phage was SCS110 from Stratagene. [γ-^{32}P]ATP (6000 Ci/mmol) was from New England Nuclear, and ATP was from Pharmacia. Acetonitrile, β-mercaptoethanol, and ammonium acetate were from Aldrich, and ammonium phosphate dibasic was from Mallinckrodt (AR grade). Polyethyleneimine-coated TLC plates and phosphoric acid were from J. T. Baker. Sephadex G-25 spin columns were from Boehringer Mannheim.

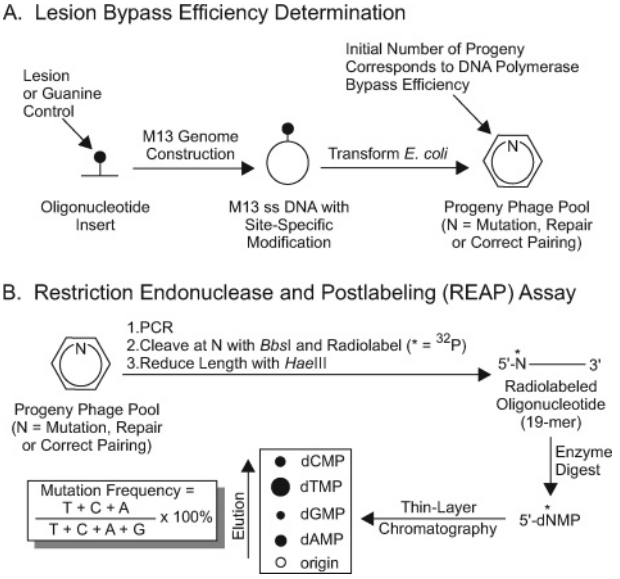

Figure 1. (A) Strategy for determination of translesion DNA polymerase bypass of base damage in vivo. A site specifically modified oligonucleotide is ligated into ss viral M13 DNA. Transfection into host cells followed by translesion DNA synthesis ultimately affords infective progeny phage whose initial numbers are limited by the lethality of the site specific lesion. Plating of the transformation mixture onto a lawn of indicator bacteria caused the formation of plaques (spots of infected cells), whose numbers allowed for the calculation of the efficiency of polymerase bypass when compared with the nonlesion control. (B) Detection of mutations using the REAP assay. PCR amplification of the region from the progeny phage that had originally contained the site specific lesion was performed for each transfection. The resulting duplex DNA was cleaved with *Bbs*I, dephosphorylated, radiolabeled at the 5′-end, and reduced in size with *Hae*III to a 19-mer. Digestion of the radiolabeled and purified 19-mer to 5′-dNMPs, separation by TLC, and quantification of the radioactivity by PhosphorImager analysis allowed measurement of the fractional composition of each base to within 1%.

Nucleosides. Treatment of 3′,5′-di-*O*-Ac-8-oxoGuo with $ONOO^-$ followed by HPLC purification allowed isolation of the Oa nucleoside derivative, as previously described (*33*).

Hydrolysis of Oa. The decomposition of Oa was followed using a coupled enzymatic spectrophotometric oxalate assay (Sigma-Aldrich or Trinity Biotech), which allowed detection of oxalate in solution through the production of an indamine dye. The oxalate kit consisted of two reagents, A [active ingredients: 3 mM 3-(dimethylamino)benzoic acid and 0.22 mM 3-methyl-2-benzothiazolinone hydrazone, pH 3.1] and B (active ingredients: 3000 U/L barley oxalate oxidase and 100000 U/L horseradish peroxidase). The following general procedure was used for the decomposition reactions: Oa (1.5 nmol) in 30 μL of buffer solution was incubated at 37 °C for a prescribed period of time. The buffer solution was pH 7.4 and consisted of 150 mM potassium phosphate and, where indicated, 5 mM magnesium sulfate and/or 20 mM sodium bicarbonate. After the incubation, 30 μL of a 2X solution of reagent A was added, followed by 12 μL of reagent B. The solution was mixed and

incubated at room temperature for 15 min, and the A_{590} of the resulting indamine dye was determined by spectrophotometry. The initial concentration of Oa was adjusted such that complete reaction to form oxalate resulted in an absorbance of 1.0 in a 1 cm path length cell.

Oligonucleotides. Oligonucleotides were from Research Genetics (Huntsville, AL), Integrated DNA Technologies (Coraville, IA), or synthesized on an Applied Biosystems model 391 DNA synthesizer. Oligonucleotides were deprotected with concentrated NH_4OH for 18 h at 55 °C. The strand containing 8-oxoG, to prevent degradation of the lesion, required 0.25 M β-mercaptoethanol in the deprotection solution. Oligonucleotides made by solid phase synthesis were purified by polyacrylamide gel electrophoresis (PAGE) and C18 reverse-phase HPLC before use (~99% purity) as described (*26*). Matrix-assisted laser desorption/ionization time-of-flight (MALDI-TOF) mass spectrometry verified the molecular weight (MW) of each strand after purification. The insert sequence was 5′-GCG AAG ACC G*X*A GCG TCC G-3′ [X = G, 8-oxoG, Oa, Ua, or a tetrahydrofuran (THF) synthetic apurinic/apyrimidinic (AP) site].

$ONOO^-$ Treatment of 8-OxoG in DNA. $ONOO^-$ was prepared by ozonation of sodium azide in alkaline solution (0.1 M NaOH) and stored at −80 °C (*34*). Concentrations of $ONOO^-$ were determined by spectrophotometry ($\epsilon = 1670\ M^{-1}\ cm^{-1}$, $\lambda = 302$ nm in 0.1 M NaOH). Reactions between $ONOO^-$ and oligonucleotides were performed in buffer containing 150 mM potassium phosphate and 25 mM sodium bicarbonate (pH 7.2), as described (*20*). The purified Oa-containing oligonucleotide was hydrolyzed to Ua under well-defined conditions as described above for the Oa nucleoside.

HPLC Purification of Modified Oligonucleotides. The Oa- and Ua-containing oligonucleotides were purified by HPLC using a 250 mm × 2.1 mm, 5 μm Supelco Supelcosil LC-18 column with UV detection at 260 nm. The mobile phase was 150 mM aqueous ammonium acetate (A) and 100% acetonitrile (B) with a gradient of 7−12% B over 30 min at a flow rate of 0.25 mL/min. The quantities of each product were calculated by UV absorbance at 260 nm using the molar absorptivity of the G-containing oligomer ($\epsilon = 184700\ M^{-1}\ cm^{-1}$) for all of the modified oligonucleotides. The mass of each oligonucleotide was determined using MALDI-TOF mass spectrometry with Oa [MW = 5843.8 (calculated), 5844.7 (observed)] and Ua [MW = 5771.8 (calculated), 5771.5 (observed)] resulting in the expected mass. The mass of each oligonucleotide was calibrated using oligonucleotides that bracketed the molecular ion of each analyte, which allowed the measured mass to routinely fall within 1 amu of the calculated mass for each lesion-containing oligonucleotide. Although a few percent of Ua contamination in the Oa sample was unavoidable, sample handling during the REAP assay either minimized or avoided additional Ua formation (*26*). Because there are relatively few products that form from 8-oxoG oxidation by $ONOO^-$ and these products are generally well-separated by HPLC purification, we are confident that the oligonucleotides were 95−99% pure.

Construction of M13 Genomes Containing a Site Specific Lesion. Single-stranded (ss) M13 genomes containing a unique lesion were generated as previously described (Figure 1A) (*26*). Briefly, 1 pmol of ss M13mp7L2 was linearized by *Eco*RI and annealed to equimolar amounts of two oligonucleotide "scaffolds," which are partially complementary to the 5′- and 3′-ends of the insert and the linearized genome. An equimolar amount of the 5′-phosphorylated 19-mer insert was added and covalently joined into the genome by incubation with T4 DNA ligase (16 °C, 1 h). The scaffolds were removed by heating (50 °C, 5 min) in the presence of a 100-fold molar excess of "anti-scaffold" complement immediately prior to transfection.

Transfection and Determination of Translesion Bypass Efficiency. Cells, grown to an $OD_{600} = 0.4$ in 100 mL of yeast tryptone (1X) medium (*35*), were made competent for transfection by the calcium chloride method as described previously (*26*, *36*). For SOS induction of bypass DNA polymerases, the cells were irradiated with 254 nm light, at an intensity of 45 J/m^2, and transferred to an equivalent volume of 2XYT media and grown for 40 min at 37 °C before being made competent. Lesion bypass was determined by transfection with 5 ng of M13 DNA, and mutation frequency was determined using 50 ng of M13 DNA. The number of independent transformed cells was determined by adding 2.5 mL of B-broth soft agar to the transfected cells and plating onto a lawn of NR9050 *E. coli*. The number of plaques on each plate was counted after incubation at 37 °C for 16 h. As a control to estimate the number of viable viral genomes that do not have an insert, a wild-type (WT) M13mp7L2 sample was exposed to the genome construction conditions, and the average number of resulting plaques was subtracted from the total formed by each insert-containing genomic construct. Transfections were performed in triplicate, and the bypass efficiency relative to the G control was calculated to within a 95% confidence interval of the mean for each lesion. A THF AP site was used as a DNA polymerase blocking control, which provided significantly fewer plaques than the G-containing insert control.

Mutation Frequency Determination. The point mutations caused by each lesion in AB1157 *E. coli* were determined and quantified using the REAP assay as previously described (Figure 1B) (*26*). Briefly, transformed cells for determination of mutation frequency were added to 10 mL of LB media and incubated on a roller drum for 5 h at 37 °C (growth), followed by pelleting of the cells and decanting of the phage-containing supernatant into new 15 mL polypropylene tubes. A 100 μL aliquot of the suspension was added to 9 mL of LB and 1 mL of mid-log SCS110 *E. coli*. The cells were incubated for 4 h (regrowth) and pelleted, and the phage-containing supernatant was decanted and stored at 4 °C. The growth and regrowth steps served to amplify the amount of progeny phage while reducing the relative amount of nontransfected DNA to a negligible amount (<0.1%). The mutation frequencies were determined by performing the REAP assay on a DNA duplex produced by PCR amplification of the insert region of the progeny phage. Each 101-mer PCR product was cleaved by *Bbs*I at the position in the template vector that originally contained the lesion, affording a 55-mer whose newly formed 5′-end contained the lesion site. The 55-mer was dephosphorylated with shrimp alkaline phosphatase, which exposed the lesion site at the 5′-OH for radiolabeling with PNK and [γ-^{32}P]ATP. Incubation with *Hae*III, to yield a 19-mer, allowed PAGE purification of the radiolabeled fragment of interest. Digestion of the desalted 19-mer to 5′-deoxynucleotide monophosphates (5′-dNMPs) with snake venom phosphodiesterase was followed by partitioning of the mixture on a polyethyleneimine TLC plate developed in saturated $(NH_4)_2HPO_4$ (adjusted to pH 6.1 with H_3PO_4). The separated radiolabeled nucleotides were quantified by PhosphorImager analysis, which provided the point mutation frequency and type at the lesion site.

Results and Discussion

Hydrolysis of Oa to form Ua. We investigated the hydrolytic stability and mutagenic potential of the 8-oxoG-derived products, Oa and Ua. The specific oxidation of an 8-oxoG-containing oligonucleotide with $ONOO^-$ followed by HPLC purification of the modified oligonucleotide was used to obtain pure Oa. The lesion Ua was observed to form via divalent metal cation and base-catalyzed hydrolysis (Scheme 1), and the identity of the lesion was established from MALDI-TOF mass spectral data as previously reported (*20*, *26*). Incubation of Oa-containing oligonucleotide in phosphate buffered solution (pH 7.4) at 37 °C caused no discernible conversion to Ua (data not shown). However, addition of Mg^{2+}, Ca^{2+}, and HCO_3^- to the solution at concentrations that are isotonic to mammalian cells, incubation in alkaline solution, or incubation in pure water at high temperature caused appreciable hydrolysis of the Oa oligonucleotide to form

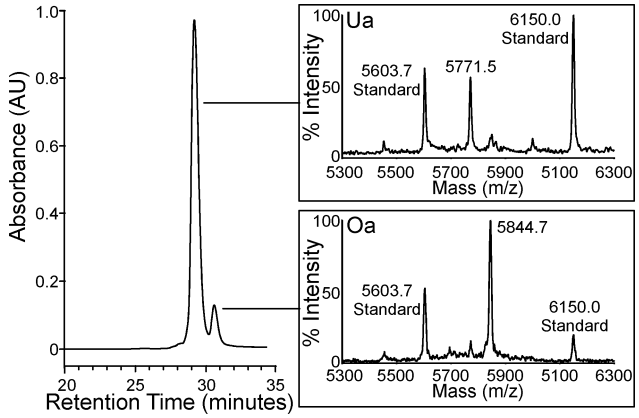

Figure 2. Hydrolysis of Oa to form Ua in an oligonucleotide. (Left) HPLC chromatogram of the Oa-containing 19-mer oligonucleotide after heating in neat H_2O for 20 min at 80 °C. (Right) MALDI-TOF mass spectra of the purified products.

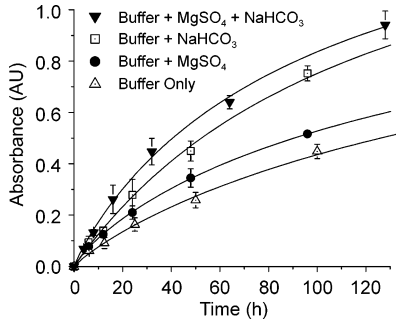

Figure 3. Oxalate formation curves for the decomposition of Oa 2′-deoxynucleoside at 37 °C in 150 mM potassium phosphate buffer, pH 7.4. Where noted, the buffer also contained 5 mM $MgSO_4$ and/or 20 mM $NaHCO_3$. The error bars represent a 95% confidence interval of the mean for three independent experiments.

a new species, which was assigned as Ua (Figure 2). The decrease in mass by 72 amu corresponds to the expected loss of oxalate during Ua formation.

As a model system to study conveniently the hydrolysis reaction under a variety of conditions, the 3′-5′-di-*O*-acetyl-2′-deoxynucleoside of Oa was synthesized from 3′,5′-di-*O*-acetyl-2′-deoxy-8-oxoguanosine (*26*, *33*). The Oa nucleoside was exposed to HCO_3^- and to various divalent alkaline earth metal cations in order to determine if these species can catalyze hydrolysis to Ua at or near in vivo concentrations. Exposure of the Oa nucleoside at 37 °C to a phosphate buffered solution containing 5 mM $MgSO_4$ and 20 mM $NaHCO_3$ (pH 7.4) resulted in almost complete hydrolysis of the nucleoside (half-life ~40 h), as determined by a commercially available oxalate assay (see Materials and Methods), whereas exposure of the Oa nucleoside to similar conditions without a divalent metal cation (half-life ~52 h) and without HCO_3^- (half-life ~96 h) resulted in much slower hydrolysis of the nucleoside starting material, with the phosphate-buffered control hydrolyzing at the slowest rate (half-life ~130 h) (Figure 3).

The addition of 5 mM $MgSO_4$ to an aqueous potassium phosphate buffered solution (pH 7.4) increased the rate of hydrolysis of the Oa nucleoside (Figure 3), implying that Mg^{2+} stabilizes the rate-determining transition state for the reaction. A previous study showed that oxalate binds Mg^{2+} effectively (*37*), and Falvello et al. recently demonstrated that the divalent metal cations Co^{2+}, Ni^{2+}, and Cu^{2+} can form a complex with the oxalate moiety of oxalurate (*38*). Thus, it is plausible that Oa also chelates Mg^{2+}. The binding of a divalent metal cation to Oa could increase the rate of hydrolysis by several mechanisms, either alone or in concert. By binding to the oxalate portion of Oa, electron density could be reduced at the carbonyl of the amide, thereby facilitating nucleophilic addition at the amide carbon. The developing negative charge on the amide carbonyl oxygen during nucleophilic addition would also be stabilized by the presence of Mg^{2+}. Divalent metal cations could also stabilize the electrostatic repulsion between the carboxylate of Oa and a negatively charged incoming nucleophile (HO^- or HCO_3^-). Alternatively, chelation of a divalent metal cation by the oxalate moiety could facilitate the elimination of this group in a manner similar to the commonly known Mg^{2+}-assisted elimination of inorganic phosphate or pyrophosphate during the hydrolysis of nucleotide triphosphates.

Surprisingly, HCO_3^- significantly increased the rate of hydrolysis of the Oa nucleoside (Figure 3). During the hydrolysis by water, a *gem*-diol tetrahedral intermediate is presumed to form at the amide carbon. The spontaneous hydrolysis of Oa may be explained through a comparison of the leaving group pK_a values. The pK_a of Ua is approximately 14 (*39*), whereas the pK_a of water is 15.7. Assuming a minimal effect on the Ua pK_a due to the 2-deoxyribose substituent, the reaction should favor elimination of Ua. If instead of hydroxide, HCO_3^- adds to the amide carbonyl of Oa, forming a tetrahedral intermediate, fragmentation would not occur directly from this structure. Collapse of the tetrahedral structure at this point should eliminate HCO_3^- (pK_a $H_2CO_3 = 6.35$) about 10^7 fold more frequently than Ua, making the fragmentation of Oa an unlikely event. However, the tetrahedral intermediate may follow a different reaction coordinate. The pK_a of HCO_3^- is 10.3; however, esterification of HCO_3^- to produce carbonic acid monomethyl ester (CH_3OCOOH) results in a significant decrease of the pK_a of the acid to 2.92 (*40*). Upon addition of HCO_3^- to Oa, it is likely that a large decrease of the carbonic acid pK_a also results. Deprotonation of the carbonic acid could conceivably initiate a decarboxylation event and subsequent fragmentation of Oa.

During the reaction of Oa with HCO_3^-, several factors may contribute to the hydrolysis rate increase. We propose that the reaction proceeds by the addition of HCO_3^- to Oa followed by decarboxylation and fragmentation (Scheme 2). Decarboxylation and fragmentation may

Scheme 2

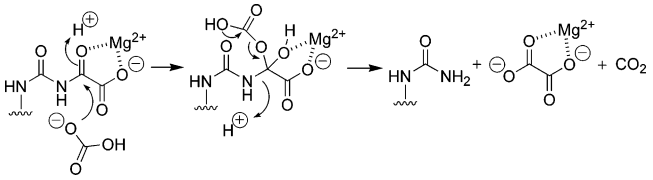

occur in a concerted fashion or in several separate steps. Herschlag and Jencks investigated a Mg^{2+}-catalyzed reaction in which carboxylate ions react with phosphorylated pyridines in a nucleophilic fashion (*41*). They found that HCO_3^- reacts much faster than CO_3^{2-}, even though CO_3^{2-} is more basic, because HCO_3^- hydrogen bonds to a phosphoryl oxygen in the transition state, thereby avoiding unfavorable electrostatic interactions. They also note that Mg^{2+} may serve as a template for the reacting species. In the present case, intramolecular

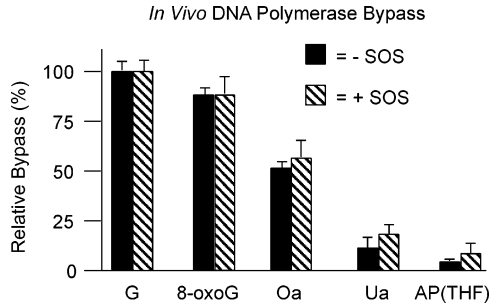

Figure 4. Relative bypass efficiency for Oa and Ua. Controls include G (well-bypassed) and a synthetic THF AP site (blocking). The error bars represent a 95% confidence interval of the mean for three independent experiments.

hydrogen bonding may contribute to the ability of HCO_3^- to react with Oa. Given the stabilizing role that Mg^{2+} appears to play during the hydrolysis of Oa in the absence of HCO_3^-, it may also play a similar role in the addition of HCO_3^- to Oa.

In Vivo Mutagenesis by Oa and Ua under Normal or SOS-Induced Conditions. The mutagenic potential of Ua was tested in vivo by inserting oligonucleotides containing each defined lesion (8-oxoG, Oa, or Ua) into M13mp7L2 ss viral genomes and then transfecting the genomes into WT *E. coli* (Figure 1). Each lesion was bypassed during replication in vivo efficiently enough to produce progeny phage for the determination of point mutation frequency and type using the REAP assay.

Because lesions in DNA may block or inhibit replication, the relative number of plaques formed from the immediate plating of the transformation mixture gives a measure of the efficiency of translesion DNA synthesis. A comparison of the number of plaques obtained after transformation of the site specific lesion-containing phage genome with that from an identically constructed vector that did not carry any oxidative damage allowed calculation of the relative bypass efficiency (*26*, *27*). As shown in Figure 4, vector survival for Oa is 51 ± 3%, which is in agreement with a previously published value (*26*). The Ua lesion bypass efficiency was 11 ± 5%, which is significantly higher that that observed for a synthetic THF AP site employed as a control for DNA polymerase blocking and SOS-induced bypass (*26*, *27*, *42*, *43*). The bypass efficiencies of the lesions were also determined in cells with the SOS system induced. Significant differences were not observed as compared to uninduced cells using the assay described in Figure 1A, as Oa and Ua were bypassed with efficiencies of 56 ± 9 and 18 ± 4%, respectively. However, increased levels of insert-containing DNA after PCR amplification during the REAP protocol were observed for Ua and THF (see Supporting Information), which is consistent with an increased bypass efficiency. The error inherent in the bypass assay does not allow small increases in bypass efficiency to be observed with statistical significance. The inefficient bypass of Ua is in accord with previous studies (*44*). Successful induction of the SOS operon is supported by the change in the mutation specificity of Ua (see below) and the increased levels of insert-containing DNA after PCR amplification of Ua and the THF lesion as compared to uninduced controls during the REAP assay (see Supporting Information).

As shown in Figure 5, in uninduced cells, the mutation frequency and type for both Oa and Ua was 99% with nearly all of the mutations in the form of G→T trans-

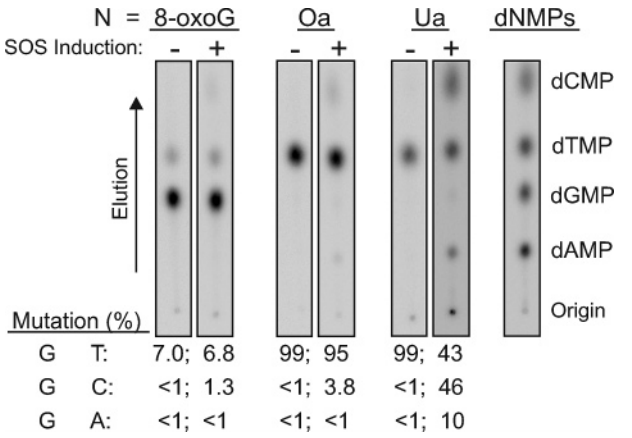

Figure 5. TLC showing mutation frequency and type as determined by the REAP assay. Markers consisting of 5′-dNMPs were derived from digestion of a 13-mer oligonucleotide that contained a degenerate 5′ terminus.

versions (based on the lesions originating from G). The mutation type and frequency for each lesion was also determined in SOS-induced cells in order to investigate the effect of inducible error-prone translesion DNA polymerase bypass on the coding properties of these lesions. As compared with normal cells, SOS induction caused Oa to have a somewhat similar mutation frequency and type, with 95% G→T and 4% G→C transversions. In contrast, the more blocking Ua had a dramatically different distribution of mutation types with 43% G→T, 46% G→C, and 10% G→A mutations and no measurable repair or correct coding. The observed insertion of G and A opposite Ua, regardless of SOS induction, is in general agreement with previous in vitro and in vivo studies (*45*−*47*). For example, Maccabee et al. reported that Ua produced from T oxidation directed insertion of G and T opposite the lesion with a frequency of 62 and 26%, respectively, as compared to other point mutations (*45*). Direct comparison of these results to the REAP data is difficult because of sequence context variations and because Ua was not introduced site specifically into the DNA, which does not allow repair or correct coding to be scored. Studies in vitro demonstrate that Ua is excised by several DNA glycosylases involved in base excision repair in *E. coli* such as Endo III, Endo VIII, and their homologues in higher organisms (*48*). Additionally, another DNA glycosylase, MutM, also known as Fpg, removes Oa in duplex DNA when the lesion is situated opposite a C (*20*).

The increase in the degeneracy of the type of nucleoside inserted opposite Ua is consistent with the larger, more flexible binding pocket generally found in Y-family lesion bypass polymerases (*49*). This binding pocket may accommodate atypical steric configurations and unfavorable electrostatic interactions induced by the lesion and allow promiscuous chain extension past the damaged DNA. Frameshifts and small deletions are assumed to be negligible in this work, since there was no detectable variation in the size of the *Bbs*I/*Hae*III restriction fragment (see Supporting Information). Clearly, the presence of Ua, like the precursor Oa, causes a higher mutation frequency in DNA than the parent 8-oxoG.

Because well-bypassed lesions (i.e., ∼50% or greater relative to guanine) have essentially no change in bypass efficiency or mutation profile with SOS induction, they are likely to be successfully replicated in *E. coli* regard-

less of SOS status. The change in coding specificity observed for Ua during SOS induction is consistent with recent models describing the initiation of a "handoff" from the replicative DNA polymerase to an error-prone bypass DNA polymerase upon encountering a lesion that stalls the replication fork (*49*). Well-bypassed lesions include not only Oa but also Ca, Iz, Oz, and Gh (Table 1). The Ua lesion exists as a mixture of α- and β-anomers, so it is intriguing to hypothesize that the α-anomer may block DNA polymerase extension until β-anomerization permits limited translesion bypass. SOS induction likely allows error-prone DNA polymerases to bypass the lesion, perhaps regardless of the anomeric state of the sugar. Further experiments are needed to elucidate the structural basis of this possible effect. NMR analysis of a duplex dodecamer containing Ua showed evidence of both anomers when placed opposite T and that the β-anomer was interhelical (aligned with the base stack) while sharing at least one hydrogen bond with the opposing nucleotide (*50*). This hydrogen-bonding interaction indicates that the lesion may be instructional, rather than simply forcing the polymerase to obey the "A" rule, which states that A will be most likely incorporated opposite a noninstructional lesion (*51*). A recent paper by Kroeger et al. (*52*) discusses application of the REAP assay to 2′-deoxyribonolactone, an AP site analogue, and proposes that even limited hydrogen bonding contributes to the lesion being instructional. We suggest that dA incorporation opposite Ua is, in part, attributable to hydrogen bonding between the carbonyl and/or distal hydrogen of the Ua moiety and the respective N6-amino and/or N1 of dA. This explanation of Ua as an instructional lesion is speculative, and alternative hydrogen-bonding patterns cannot be ruled out, particularly for SOS-induced lesion bypass. Another explanation that is consistent with a recent report by Kobayashi et al. is that nucleotide insertion opposite Ua is inhibited, resulting in slippage and insertion of a second nucleotide opposite the base on the 3′-side of the template Ua (*53*). However, the local sequence used in our work [5′-G(Ua)A-3′] only allows for G→A mutations to occur by this mechanism, and these mutations are only observed to a modest degree during SOS induction as compared to the predominant G→T and G→C mutations.

The 8-oxoG-derived DNA lesions Oa and Ua are mutagenic under normal and SOS-induced conditions in vivo. If these lesions form in cells, they clearly represent a threat to genomic integrity in the absence of an effective DNA repair mechanism.

Acknowledgment. We thank Dr. Kaushik Mitra for helpful discussions on the mechanism of Oa hydrolysis. This work was supported by the National Institutes of Health (CA86489, ES07020, and CA26731) and by the California Breast Cancer Research Program (9KB-0179). This work was performed, in part, under the auspices of the U.S. Department of Energy by the University of California, Lawrence Livermore National Laboratory, under Contract No. W-7405-Eng-48.

Supporting Information Available: Agarose and polyacrylamide gels from the REAP assay; HPLC chromatograms and mass spectra of Oa and Ua nucleosides. This material is available free of charge via the Internet at http://pubs.acs.org.

References

(1) Beckman, K. B., and Ames, B. N. (1997) Oxidative decay of DNA. *J. Biol. Chem. 272*, 19633−19636.

(2) Dedon, P. C., and Tannenbaum, S. R. (2004) Reactive nitrogen species in the chemical biology of inflammation. *Arch. Biochem. Biophys. 423*, 12−22.

(3) Marnett, L. J. (2000) Oxyradicals and DNA damage. *Carcinogenesis 21*, 361−370.

(4) Dizdaroglu, M. (1992) Oxidative damage to DNA in mammalian chromatin. *Mutat. Res. 275*, 331−342.

(5) Grollman, A. P., and Moriya, M. (1993) Mutagenesis by 8-oxoguanine: An enemy within. *Trends Genet. 9*, 246−249.

(6) Helbock, H. J., Beckman, K. B., and Ames, B. N. (1999) 8-Hydroxydeoxyguanosine and 8-hydroxyguanine as biomarkers of oxidative DNA damage. *Methods Enzymol. 300*, 156−166.

(7) Moriya, M., Ou, C., Bodepudi, V., Johnson, F., Takeshita, M., and Grollman, A. P. (1991) Site-specific mutagenesis using a gapped duplex vector: A study of translesion synthesis past 8-oxodeoxyguanosine in E. coli. *Mutat. Res. 254*, 281−288.

(8) Wood, M. L., Esteve, A., Morningstar, M. L., Kuziemko, G. M., and Essigmann, J. M. (1992) Genetic effects of oxidative DNA damage: Comparative mutagenesis of 7,8-dihydro-8-oxoguanine and 7,8-dihydro-8-oxoadenine in *Escherichia coli*. *Nucleic Acids Res. 20*, 6023−6032.

(9) Wood, M. L., Dizdaroglu, M., Gajewski, E., and Essigmann, J. M. (1990) Mechanistic studies of ionizing radiation and oxidative mutagenesis: Genetic effects of a single 8-hydroxyguanine (7-hydro-8-oxoguanine) residue inserted at a unique site in a viral genome. *Biochemistry 29*, 7024−7032.

(10) Steenken, S., and Jovanovic, S. V. (1997) How easily oxidizable is DNA? One-electron reduction potentials of adenosine and guanosine radicals in aqueous solution. *J. Am. Chem. Soc. 119*, 617−618.

(11) Adam, W., Arnold, M. A., Gruene, M., Nau, W. M., Pischel, U., and Saha-Moeller, C. R. (2002) Spiroiminodihydantoin is a major product in the photooxidation of 2′-deoxyguanosine by the triplet states and oxyl radicals generated from hydroxyacetophenone photolysis and dioxetane thermolysis. *Org. Lett. 4*, 537−540.

(12) Burrows, C. J., and Muller, J. G. (1998) Oxidative nucleobase modifications leading to strand scission. *Chem. Rev. 98*, 1109−1152.

(13) Cullis, P. M., Malone, M. E., and Merson-Davies, L. A. (1996) Guanine radical cations are precursors of 7,8-dihydro-8-oxo-2′-deoxyguanosine but are not precursors of immediate strand breaks in DNA. *J. Am. Chem. Soc. 118*, 2775−2781.

(14) Kino, K., and Sugiyama, H. (2001) Possible cause of G−C→C−G transversion mutation by guanine oxidation product, imidazolone. *Chem. Biol. 8*, 369−378.

(15) Luo, W., Muller, J. G., Rachlin, E. M., and Burrows, C. J. (2000) Characterization of spiroiminodihydantoin as a product of one-electron oxidation of 8-oxo-7,8-dihydroguanosine. *Org. Lett. 2*, 613−616.

(16) Luo, W., Muller, J. G., Rachlin, E. M., and Burrows, C. J. (2001) Characterization of hydantoin products from one-electron oxidation of 8-oxo-7,8-dihydroguanosine in a nucleoside model. *Chem. Res. Toxicol. 14*, 927−938.

(17) Niles, J. C., Wishnok, J. S., and Tannenbaum, S. R. (2000) A novel nitration product formed during the reaction of peroxynitrite with 2′,3′,5′-tri-O-acetyl-7,8-dihydro-8-oxoguanosine: N-Nitro-N′-[1-(2,3,5-tri-O-acetyl-beta-D-erythro-pentofuranosyl)-2,4-dioxo-imidazolidin-5-ylidene]guanidine. *Chem. Res. Toxicol. 13*, 390−396.

(18) Niles, J. C., Wishnok, J. S., and Tannenbaum, S. R. (2001) A novel nitroimidazole compound formed during the reaction of peroxynitrite with 2′,3′,5′-tri-O-acetyl-guanosine. *J. Am. Chem. Soc. 123*, 12147−12151.

(19) Niles, J. C., Wishnok, J. S., and Tannenbaum, S. R. (2001) Spiroiminodihydantoin is the major product of the 8-oxo-7,8-dihydroguanosine reaction with peroxynitrite in the presence of thiols and guanosine photooxidation by methylene blue. *Org. Lett. 3*, 963−966.

(20) Tretyakova, N. Y., Niles, J. C., Burney, S., Wishnok, J. S., and Tannenbaum, S. R. (1999) Peroxynitrite-induced reactions of synthetic oligonucleotides containing 8-oxoguanine. *Chem. Res. Toxicol. 12*, 459−466.

(21) Uppu, R. M., Cueto, R., Squadrito, G. L., Salgo, M. G., and Pryor, W. A. (1996) Competitive reactions of peroxynitrite with 2′-deoxyguanosine and 7,8-dihydro-8-oxo-2′-deoxyguanosine (8-oxodG): Relevance to the formation of 8-oxodG in DNA exposed to peroxynitrite. *Free Radical Biol. Med. 21*, 407−411.

(22) Burney, S., Caulfield, J. L., Niles, J. C., Wishnok, J. S., and Tannenbaum, S. R. (1999) The chemistry of DNA damage from nitric oxide and peroxynitrite. *Mutat. Res. 424*, 37−49.

(23) Carreras, M. C., Pargament, G. A., Catz, S. D., Poderoso, J. J., and Boveris, A. (1994) Kinetics of nitric oxide and hydrogen

peroxide production and formation of peroxynitrite during the respiratory burst of human neutrophils. *FEBS Lett. 341*, 65−68.
(24) Xia, Y., and Zweier, J. L. (1997) Superoxide and peroxynitrite generation from inducible nitric oxide synthase in macrophages. *Proc. Natl. Acad. Sci. U.S.A. 94*, 6954−6958.
(25) Niles, J. C., Wishnok, J. S., and Tannenbaum, S. R. (2004) Spiroiminodihydantoin and guanidinohydantoin are the dominant products of 8-oxoguanosine oxidation at low fluxes of peroxynitrite: Mechanistic studies with ^{18}O. *Chem. Res. Toxicol. 17*, 1510−1519.
(26) Henderson, P. T., Delaney, J. C., Gu, F., Tannenbaum, S. R., and Essigmann, J. M. (2002) Oxidation of 7,8-dihydro-8-oxoguanine affords lesions that are potent sources of replication errors in vivo. *Biochemistry 41*, 914−921.
(27) Henderson, P. T., Delaney, J. C., Muller, J. G., Neeley, W. L., Tannenbaum, S. R., Burrows, C. J., and Essigmann, J. M. (2003) The hydantoin lesions formed from oxidation of 7,8-dihydro-8-oxoguanine are potent sources of replication errors in vivo. *Biochemistry 42*, 9257−9262.
(28) Neeley, W. L., Delaney, J. C., Henderson, P. T., and Essigmann, J. M. (2004) In vivo bypass efficiencies and mutational signatures of the guanine oxidation products 2-aminoimidazolone and 5-guanidino-4-nitroimidazole. *J. Biol. Chem. 279*, 43568−43573.
(29) Hosford, M. E., Muller, J. G., and Burrows, C. J. (2004) Spermine participates in oxidative damage of guanosine and 8-oxoguanosine leading to deoxyribosylurea formation. *J. Am. Chem. Soc. 126*, 9540−9541.
(30) Delaney, J. C., and Essigmann, J. M. (1999) Context-dependent mutagenesis by DNA lesions. *Chem. Biol. 6*, 743−753.
(31) Delaney, J. C., and Essigmann, J. M. (2001) Effect of sequence context on O(6)-methylguanine repair and replication in vivo. *Biochemistry 40*, 14968−14975.
(32) Delaney, J. C., Henderson, P. T., Helquist, S. A., Morales, J. C., Essigmann, J. M., and Kool, E. T. (2003) High-fidelity in vivo replication of DNA base shape mimics without Watson−Crick hydrogen bonds. *Proc. Natl. Acad. Sci. U.S.A. 100*, 4469−4473.
(33) Niles, J. C., Burney, S., Singh, S. P., Wishnok, J. S., and Tannenbaum, S. R. (1999) Peroxynitrite reaction products of 3′,5′-di-O-acetyl-8-oxo-7,8-dihydro-2′-deoxyguanosine. *Proc. Natl. Acad. Sci. U.S.A. 96*, 11729−11734.
(34) Pryor, W. A., Cueto, R., Jin, X., Koppenol, W. H., Ngu-Schwemlein, M., Squadrito, G. L., Uppu, P. L., and Uppu, R. M. (1995) A practical method for preparing peroxynitrite solutions of low ionic strength and free of hydrogen peroxide. *Free Radical Biol. Med. 18*, 75−83.
(35) Miller, J. H. *A Short Course in Bacterial Genetics: A Laboratory Manual and Handbook for Escherichia coli and Related Bacteria* (1992) Cold Spring Harbor Laboratory, New York.
(36) Banerjee, S. K., Borden, A., Christensen, R. B., LeClerc, J. E., and Lawrence, C. W. (1990) SOS-dependent replication past a single trans-syn T−T cyclobutane dimer gives a different mutation spectrum and increased error rate compared with replication past this lesion in uninduced cells. *J. Bacteriol. 172*, 2105−2112.
(37) Watanabe, S., Trosper, T., Lynn, M., and Evenson, L. (1963) The magnesium binding constants of adenosinetriphosphate and some other compounds estimated by the use of fluorescence of magnesium-8-hydroxyquinoline. *J. Biochem. (Tokyo) 54*, 17−24.
(38) Falvello, L. R., Garde, R., and Tomas, M. (2002) Flexible square supramolecular rings with hydrogen-bonded bushing in solid-state oxalurate complexes: Versatility of the oxalurate ligand in covalent and noncovalent binding. *Inorg. Chem. 41*, 4599−4604.
(39) Woolley, E. M., and Hepler, L. G. (1972) Apparent ionization constants of water in aqueous organic mixtures and acid dissociation constants of protonated cosolvents in aqueous solution. *Anal. Chem. 44*, 1520−1523.
(40) Guthrie, J. P. (1978) Hydrolysis of esters of oxy acids: pK_a values for strong acids; Bronsted relationship for attack of water at methyl; free energies of hydrolysis of esters of oxy acids; and a linear relationship between free energy of hydrolysis and pK_a holding over a range of 20 pK units. *Can. J. Chem. 56*, 2342−2354.
(41) Herschlag, D., and Jencks, W. P. (1990) The effects of magnesium2+, hydrogen bonding, and steric factors on rate and equilibrium constants for phosphoryl transfer between carboxylate ions and pyridines. *J. Am. Chem. Soc. 112*, 1942−1950.
(42) Lawrence, C. W., Borden, A., Banerjee, S. K., and LeClerc, J. E. (1990) Mutation frequency and spectrum resulting from a single abasic site in a single-stranded vector. *Nucleic Acids Res. 18*, 2153−2157.
(43) Reuven, N. B., Tomer, G., and Livneh, Z. (1998) The mutagenesis proteins UmuD′ and UmuC prevent lethal frameshifts while increasing base substitution mutations. *Mol. Cell 2*, 191−199.
(44) Ide, H., Kow, Y. W., and Wallace, S. S. (1985) Thymine glycols and urea residues in M13 DNA constitute replicative blocks in vitro. *Nucleic Acids Res. 13*, 8035−8052.
(45) Maccabee, M., Evans, J. S., Glackin, M. P., Hatahet, Z., and Wallace, S. S. (1994) Pyrimidine ring fragmentation products. Effects of lesion structure and sequence context on mutagenesis. *J. Mol. Biol. 236*, 514−530.
(46) McNulty, J. M., Jerkovic, B., Bolton, P. H., and Basu, A. K. (1998) Replication inhibition and miscoding properties of DNA templates containing a site-specific cis-thymine glycol or urea residue. *Chem. Res. Toxicol. 11*, 666−673.
(47) Wallace, S. S. (2002) Biological consequences of free radical-damaged DNA bases. *Free Radical Biol. Med. 33*, 1−14.
(48) Friedberg, E. C., Walker, G. C., and Siede, W. *DNA Repair and Mutagenesis* (1995) American Society for Microbiology, Washington, DC.
(49) Goodman, M. F. (2002) Error-prone repair DNA polymerases in prokaryotes and eukaryotes. *Annu. Rev. Biochem. 71*, 17−50.
(50) Gervais, V., Guy, A., Teoule, R., and Fazakerley, G. V. (1992) Solution conformation of an oligonucleotide containing a urea deoxyribose residue in front of a thymine. *Nucleic Acids Res. 20*, 6455−6460.
(51) Taylor, J. S. (2002) New structural and mechanistic insight into the A-rule and the instructional and noninstructional behavior of DNA photoproducts and other lesions. *Mutat. Res. 510*, 55−70.
(52) Kroeger, K. M., Jiang, Y. L., Kow, Y. W., Goodman, M. F., and Greenberg, M. M. (2004) Mutagenic effects of 2-deoxyribonolactone in *Escherichia coli*. An abasic lesion that disobeys the A-rule. *Biochemistry 43*, 6723−6733.
(53) Kobayashi, S., Valentine, M. R., Pham, P., O'Donnell, M., and Goodman, M. F. (2002) Fidelity of *Escherichia coli* DNA polymerase IV. Preferential generation of small deletion mutations by dNTP-stabilized misalignment. *J. Biol. Chem. 277*, 34198−34207.

TX049757K